

and 22%. Based on these data, the specimen for cyclic triaxial test was prepared with dry density and water content of 16 kN/m^3 and 20%, respectively. On the other hand, the soil block model for the shaking table test was prepared with dry density and water content of 15 kN/m^3 and 28%, respectively. The reason for conducting the cyclic triaxial test and the shaking table test with a slightly different soil compaction state is mainly because these projects were conducted to develop the dynamic testing apparatus at the authors' institution and to test their reliability, as discussed earlier. Further works are in progress but in this paper an analysis is made on the shear modulus versus the shear strain relationship of the Alam Impian residual soil based on currently available experimental results.

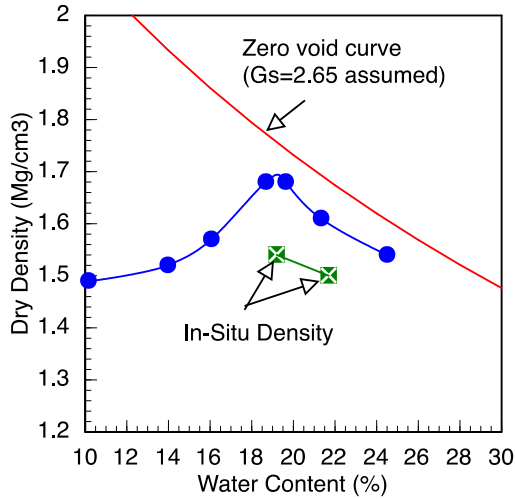


Figure 2 Compaction properties of residual soil

3. CYCLIC TRIAXIAL TEST

3.1 Testing Apparatus & Programs

Compacted specimens of 10cm diameter by 20cm height were subjected to a series of cyclic triaxial tests using the apparatus shown in Figures 3 (a) & (b).

As can be seen from Fig. 3(b), the apparatus is equipped with a load cell which is directly connected to the top cap of the specimen to measure the axial force internally within the cell to avoid the effect of shaft friction. The capacity of load cell is designed for the stress level only applicable to cyclic loading and not for loading the specimen to failure. Therefore the resolution of axial stress changes measured is very high. For controlling the cyclic loading level and frequency, a system of Electro-Pneumatic (E/P) regulator and a computer equipped with D/A converter is developed.

The specimen is prepared by statically compacting the residual soil in a mold using a hydraulic press to achieve the dry density of specimen to 16 kN/m^3 at a water content of 20%. The specimen is then consolidated to 100 kN/m^2 isotropically in the triaxial cell by monitoring the load on the internal load cell. Since the load cell is rigidly connected to the axial rod and also to the loading piston of bellofram cylinder, the isotropic consolidation requires adjustments to the air pressure at bellofram cylinder so that no change of force measured at the internal load cell. After the isotropic consolidation, the specimen is then subjected to the cyclic deviator stress of various stress levels and loading frequencies. The stress level applied varied from 0.01 to 0.3 times of the confining pressure, and the frequency varied from 0.1 to 1 Hz. Application of these different loading levels through consolidation and cyclic loading, and the frequencies applied during cyclic loading were managed by controlling the air pressure to a bellofram cylinder placed at the top of the triaxial apparatus through a system of Electro-Pneumatic (E/P) regulator and a computer equipped with D/A converter.

To measure the axial deformation of the specimen, a Linear Variable Differential Transformer (LVDT) was attached externally to measure the overall deformation, and a local displacement transducer (LDT) was attached to the specimen to measure the strain locally. Only one unit of LDT was used to measure the local strain at one side of the specimen in this study although the LDT measurements at both sides are preferable. Also, the output voltage response of the LDT was not linearly correlated with displacement and therefore the measurement accuracy depended highly on the precision of the LDT attached to the sidewall. As will be described later, the shear modulus, G , evaluated directly through the LDT measurement is judged to be valid only for the small strain range below 10^{-3} and further refinements of small strain measurement technique is necessary at our institution.

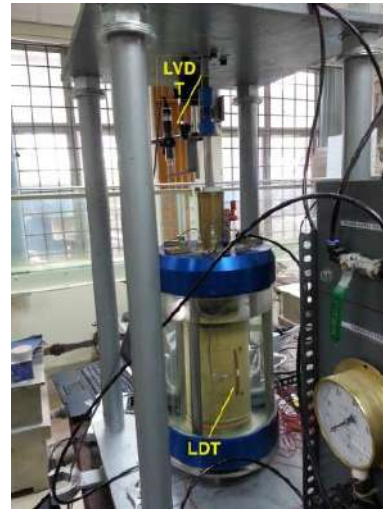


Figure 3(a) Outline view of cyclic triaxial apparatus

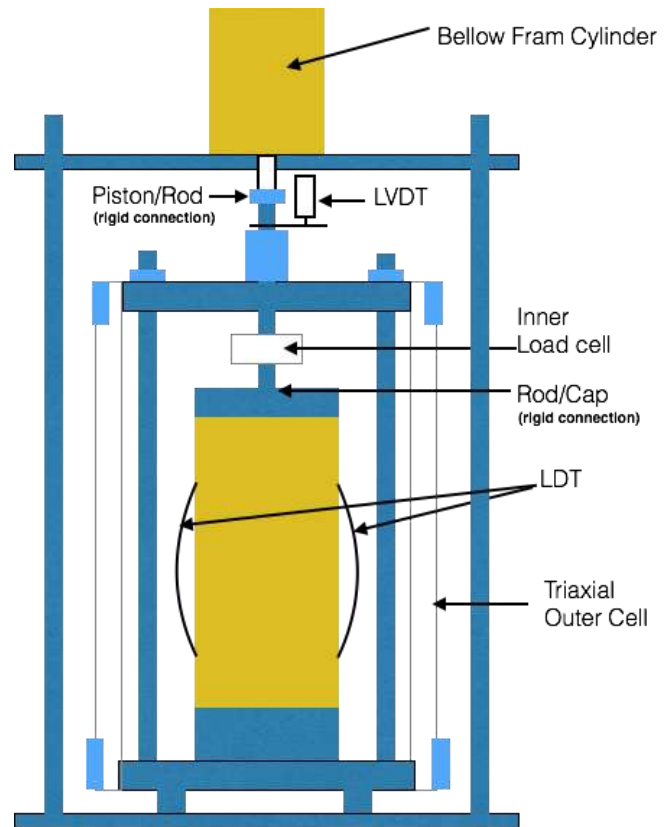
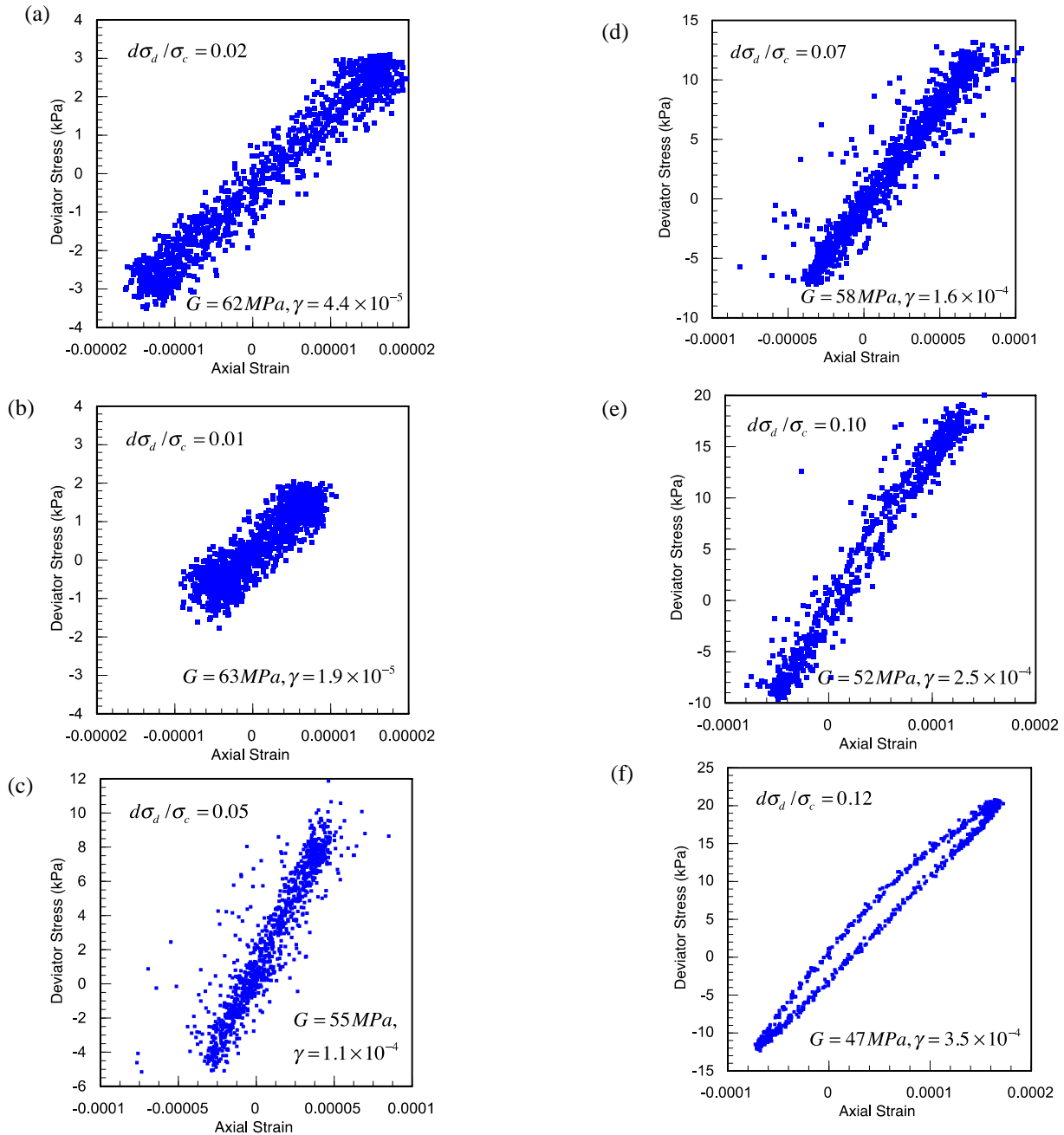


Figure 3(b) Schematic of cyclic triaxial cell with LDT & LVDT

3.2 Evaluation of Shear Modulus

strain loop are shown in Figure 4 that are based on the LDT measurements corresponding to the results obtained at the deviator stress level of 1 to 12% of the confining pressure. Although the level of cyclic deviator stress was controlled by the electronic air regulator, the actual stress level measured was slightly higher than planned. The LVDT measurements for this stress range were not accurate enough to depict useful stress-strain loops. As can be seen from Figure 4, the loops at very small stress level (1% to 7%) show

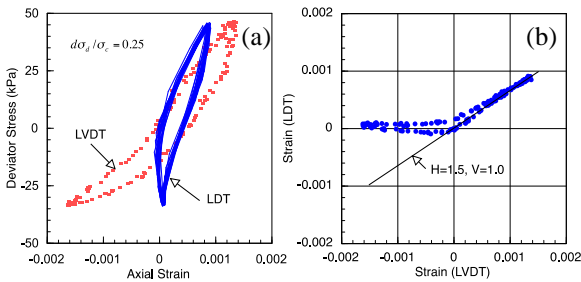
The axial deformations measured from both LVDT and LDT were used to depict the cyclic stress-strain loop to evaluate the shear modulus, G . Typical examples of such deviator stress versus axial strain some scatter but the shear modulus still can be evaluated from the average inclination of the loops. Although the tests have been carried out by increasing the loading frequency, only the results from the lowest frequency of 0.1Hz were analysed since the data from higher frequencies did not have sufficient data points such as those shown in Figure 4. The data logger used in this study had a limited scanning speed for acquiring satisfactory data points for the tests with higher frequencies.



Figures 4(a) to (f) Stress-Strain Relationships Obtained from Cyclic Triaxial Test (based on LDT measurements)

As the stress level was increased, the reliability of the LDT measurement decreased as noted earlier. Figure 5(a) shows a comparison of stress-strain loops between LVDT and LDT measurements at the stress level of 25%. Figure 5(b) depicts a direct comparison of the measured strains between LDT and LVDT. These figures clearly show that the local strain measured by LDT was much smaller than that of external LVDT measurement because the latter includes the bedding errors between the soil specimen and contacting elements, such as filter papers and porous stones, etc. The external measurement was found to be approximately 1.5 times larger than that measured by LDT. However, it was found that the response of LDT during extension loading at higher stress level (i.e., greater than 20%) were unreliable, and Figure 5(b) shows that the LDT in extension loading is not increasing while the G value at two stress levels (20% and 25%) was made using the LVDT reading by reducing its value by 2/3.

The variation of the G value with shear strain is depicted in Figure 6 using the results both from LDT and LVDT. It is clearly seen that the G value decreases with the shear strain and there is a consistent trend of G versus relationship between the results based on LDT and LVDT. The maximum value of G can be estimated to be around 64MPa, and this value corresponds to a shear wave velocity of 200m/s with the density of 1.6 Mg/m³, which seems to be a reasonable value.



Figures 5 (a) & (b) Comparison of strains measured between LDT and LVDT

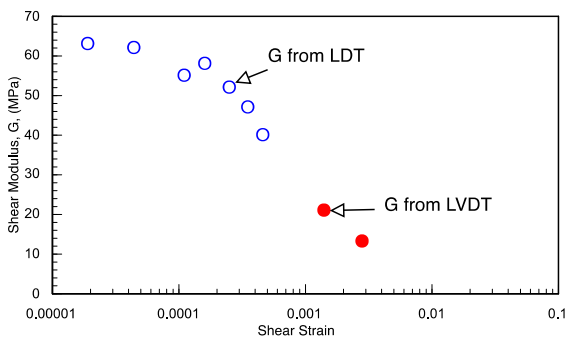


Figure 6 Variation of shear modulus with shear strain (cyclic triaxial test)

4. SHAKING TABLE TEST

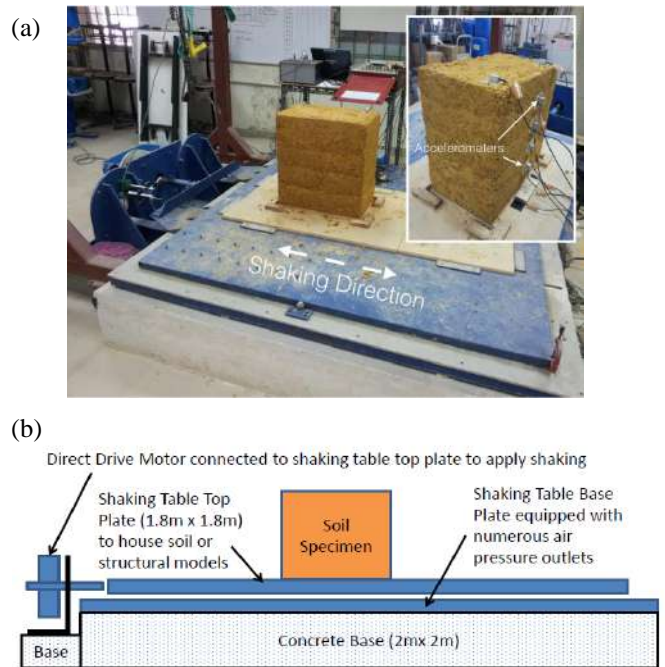
4.1 Testing Apparatus & Programs

Figure 7 shows the shaking table apparatus and the soil block model with accelerometers attached. The shaking table has a size of 2 m by 2 m where a structural model can be placed. The shaking table is air-lifted through the aluminum floor beneath the shaking table, and the maximum vertical load that can be placed on the table depends on the air-pressure supplied. When nominal air-pressure of 1 to 2 bar is

used, the vertical load of 2 to 4 tones can be placed easily on the table. The object on the table can be subjected to only one directional shaking, and a direct drive motor placed at the table end controls the rate and amount of horizontal displacement.

The acceleration force that can be generated by this shaking table apparatus depends on a combination of the amount of horizontal displacement and the frequency of shaking. For the shaking with slow frequency, a large horizontal displacement, up to 100mm, can be applied, but for the shaking with higher frequency (maximum of 25Hz), a small displacement of 1-2 mm can be applied. Usually accelerations ranging from 100 to 200 gals can be applied by this apparatus.

A research project of examining a soil-structure interaction using small model structure and ground was carried out using the same residual soil with this shaking table apparatus. In selecting the soil condition that is suitable for achieving the resonance of structural model with ground, it was decided to prepare a soil ground having a shear velocity of 50m/s. To measure the shear velocity of the residual soil, a seismic test was conducted on a 50cm high compacted residual soil column to which a pair of accelerometers were attached. The density and the water content of the soil were varied. From this test, it was found that a soil block of this residual soil with the density of 15kN/m³ and the water content of 28% would yield the desired shear velocity of 50m/s. Thus a soil block model of 50cm high, 50cm wide, and 60cm long was constructed by compacting the residual soil in a mold. The acceleration was measured at six levels, from base to top of the soil model with an interval of 10cm, as shown in Figure 7. The shaking test was conducted on the soil model only prior to adding the model structure on it, and a combination of horizontal displacements (1mm to 5mm) and frequencies (1Hz to 25Hz) were applied to the model. The measured results from this test were used herein to analyse the deformation properties of the soil model.



Figures 7 (a) Outline of shaking table test with a soil block model, (b) Schematic of shaking table test apparatus

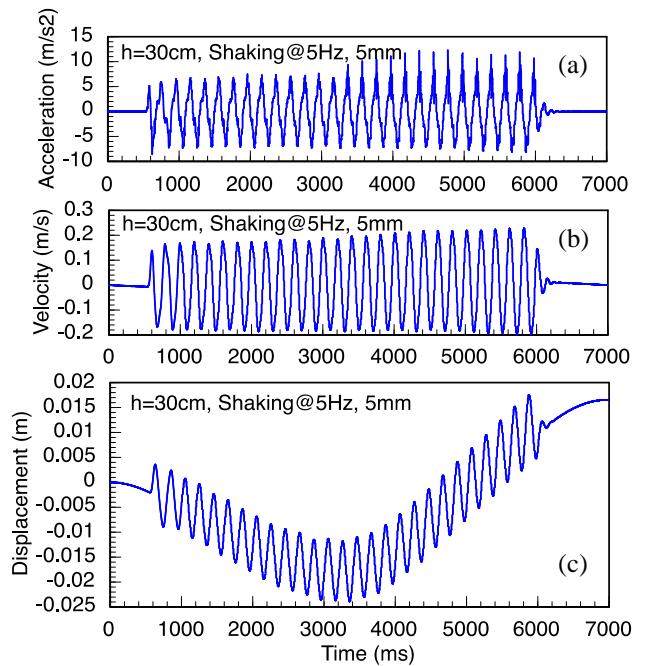
4.2 Evaluation of Shear Modulus

The procedures of evaluating the G value by obtaining the hysteresis loop between shear stress and shear strain were similar to that of the cyclic triaxial test. However, the accelerometer readings were used to compute the horizontal displacement of soil model at various heights by double integrating the measured acceleration with respect to time. The shear strain can be computed from those computed horizontal displacements between two desired heights. The shear stress can be evaluated by computing the shear force acting on the desired plane as a product of a mass of soil above that plane times the acceleration measured (Kazama et al. 1996).

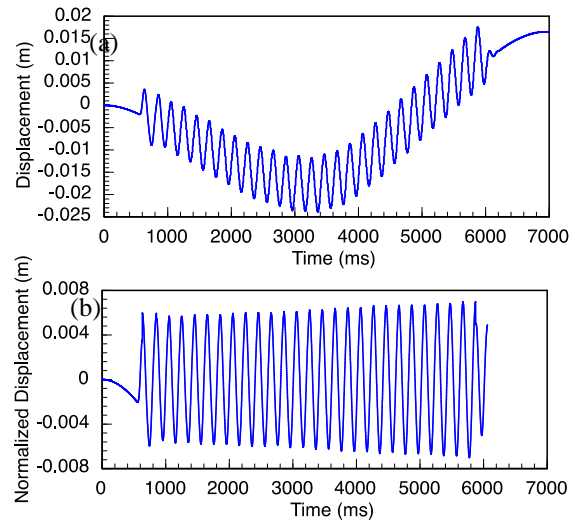
In this study, accelerations were measured at six elevations (10 cm intervals from the base to the top of 50cm high) and therefore a number of stress-strain loops based on different combinations of measured heights can be computed. Through some exploratory computations, it was decided to compute the stress-strain loops for two sets of elevations. One was the strain between the elevations 10 cm and 30 cm, and the other was that between the elevations of 10 cm and the base. An example of computing the horizontal displacement at each sensor is shown in Figures 8 and 9. In Figure 8, the measured acceleration, and the computed velocity and displacement after applying a baseline correction are shown at the top, middle, and the bottom respectively. This baseline correction to the acceleration measurement is customarily applied for field seismometer measurements to maintain a physical consistency of sensor's velocity to become zero at the end of shaking. In this study, a baseline correction method proposed by Osaki (1994) was used. However as shown in Figure 8(c), the computed displacements after the baseline correction usually show some waving trend with respect its center of oscillation.

The accuracy of baseline correction may depend on a precision of sensor placement on a horizontal plane and soil movement around the sensor. As the computed displacements after the baseline correction showed inconsistent waving trend as shown in Figure 8(c), evaluation of shear strain directly from the computed displacement becomes difficult. Therefore it was decided to normalize all computed displacements with respect to its center of oscillation in each cycle by identifying a trend line of average between the maximum and the minimum displacements in each half cycle and then normalize the data within that half cycle with respect to the trend line. Figure 10 shows such normalized displacement and the obtained symmetrical movement of soil with reference to the trend line.

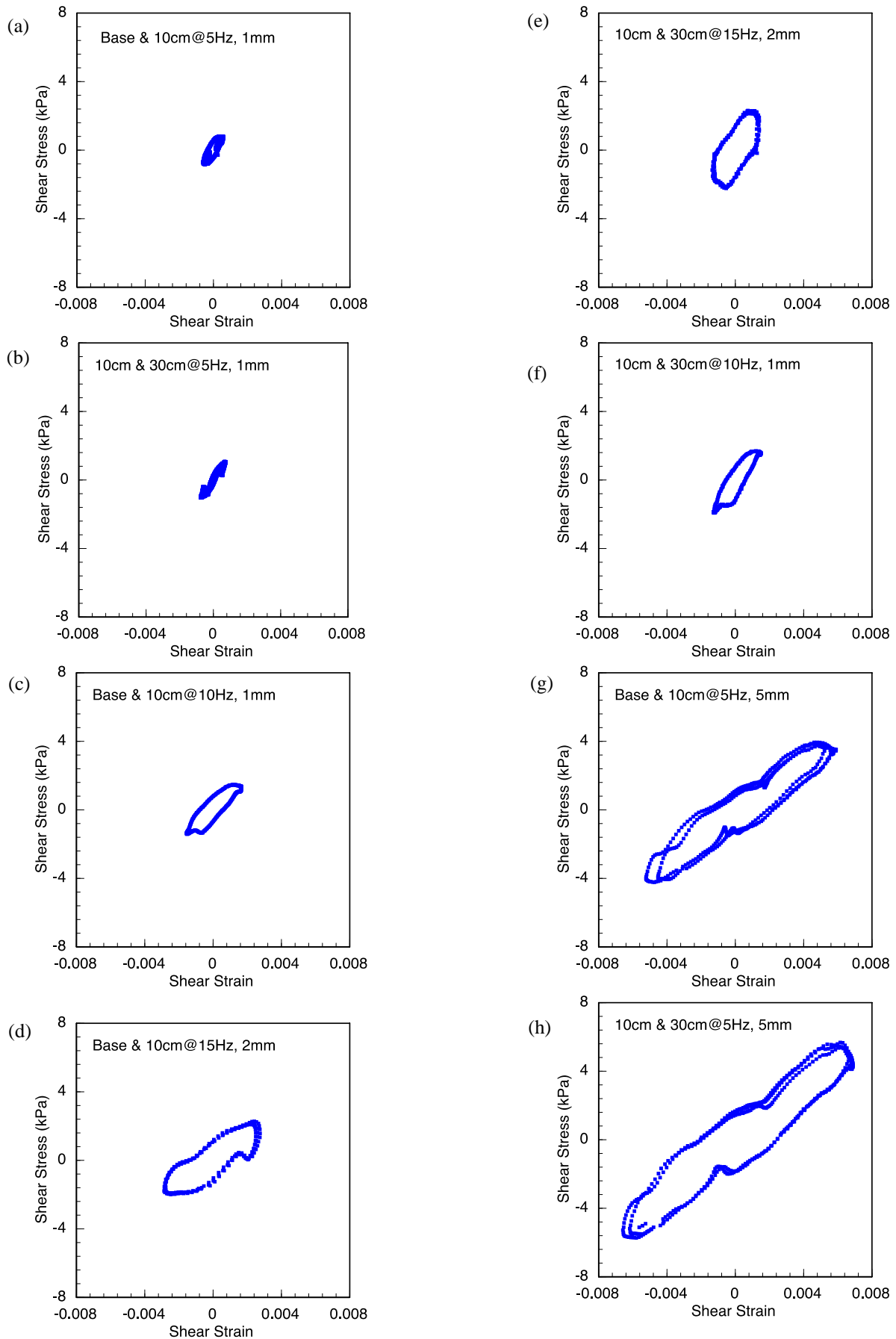
After such correction of measured data, the hysteresis loop of shear stress and shear strain were obtained for all four series of shakings (i.e., 5Hz@1mm to 15Hz@2mm) as shown in Figure 10. The stress-strain loops is the smallest for the test with 5Hz@1mm, and the largest for one with 5Hz@5mm, and this indicate the amount of horizontal displacement imposed during shaking affects strongly the intensity of shaking. From these hysteresis loops, the values of G are calculated and then normalized using the maximum shear modulus, G_0 , that can be computed from the initial setting of the soil model having a shear wave velocity of 50m/s. Figure 11 shows the variation of G/G_0 with shear strain and it also shows the normalized shear modulus from the cyclic triaxial test. In normalising the G value for the latter, the G_0 value of 64MPa is assumed as discussed earlier. The comparison between two test results shows that the changes of G/G_0 with shear strain is very similar, although the absolute values of G are quite different as the confining pressures for these two tests are vastly different. It is well known that the variation of G/G_0 with shear strain is affected dominantly by the confining pressure for sandy soil (Iwasaki et al. 1978, Kokusho 1980), while it is affected by the plasticity index for clayey soil (Vucetic and Dobry, 1991). From Figure 11, the tested residual soil may be exhibiting a dynamic property similar to those of clayey soil. More discussions on the test results will be made in the following section.



Figures 8 (a), (b), (c) Samples of computed velocity and displacement from the measured acceleration after baseline correction (Shaking 5Hz, 5mm, Sensor Height=30cm)



Figures 9 (a) Computed displacement after baseline correction, (b) Normalized displacement with respect to the trend line of oscillation centers (Shaking 5Hz, 5mm, Sensor Height=30cm)



Figures 10 (a) to (h) Hysteresis loops of shear stress and shear strain based on shaking table test

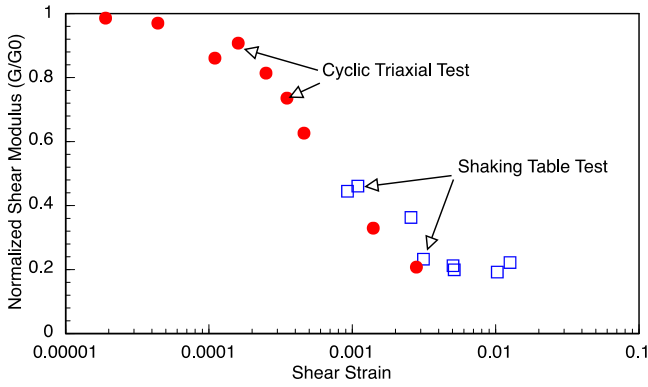


Figure 11 Variation of normalised shear modulus with shear strain

5. RESULT & DISCUSSION

The degradation of shear modulus with shear strain has been studied extensively for either purely sandy soil or clayey soil separately (Iwasaki et al. 1978, Kokusho 1980, Vucetic and Dobry, 1991). Recent researches on modeling the degradation curve have also been made by separating the materials into two (Vardanega and Bolton, 2013, Oztoprak and Bolton, 2013). As noted earlier, the residual soils in tropical region are generally formed by a mixture of sand and clay, and to complicate the matter further it is usually in unsaturated state. Studies on the shear modulus of unsaturated residual soil showed that the increase of suction increases the shear stiffness (Wong et al. 2014 and Chan 2002). The residual soil tested in this study had relatively high water contents of 20% to 28%, corresponding to the degree of saturation of 80 to 97%. In addition, the fines content was lower (less than 20%) than those Hong Kong residual soil (higher than 50%) reported for the above unsaturated soil studies (Wong et al. 2014 and Chan 2002). Thus the following discussions will proceed without considering the effect of suction on the shear stiffness, and concentrate on whether the residual soil behaves as sandy or clayey soil.

The degradation curve of shear modulus for the residual soil in Singapore has been studied by using the local strain measurement and also the bender element test (Tou, 2003, Leong, et al. 2003). Tou (2003) reported results of cyclic triaxial tests on residual soils originated from granite, namely the Bukit Timah granite, and sedimentary rock, namely the Jurong formation. The Jurong formation is a typical deposit of sedimentary rock in Singapore (Rahardjo et al. 2004) which has the same geological age as that of the Kenny Hill formation. There is however a large difference in the particle distribution between these two residual soils, although the soils are from similar sedimentary rocks. The Jurong formation soil tested by Tou (2003) and Leong et al. (2003) have higher fines content of 60 to 70%, while the Kenney Hill formation soil in the present study has much lesser fines content (< 20%). Figure 12 shows a comparison of normalized shear modulus, G/G_0 between the present experimental result and the cyclic triaxial tests performed by Tou (2003) at a confining pressure of 100kPa with 0.1Hz loading. Also shown in the figure are the data points of the normalized shear modulus obtained from the weathered granite residual soil. It may be noted that Tou (2003) obtained the maximum shear moduli for those residual soils by using the bender element test.

From the Figure 12, it is clear that the normalized shear modulus versus the shear strain relationship for the residual soils from similar sedimentary rocks in Malaysia Peninsula and Singapore is significantly different. The result of the weathered granite soil is closer to the results of this study, and the granite soil had a fines content of 37% which is much lesser than that of the Jurong sedimentary rock formation. An obvious conclusion from the comparison is that the physical soil properties such as the gradation have a more significant influence on the shear modulus versus the shear strain relationship than the parent rock origins of the soil. The

physical and mechanical behaviors of residual soil, in turn, are significantly influenced by the degree of weathering on the parent rock. Therefore, more compilation of data are necessary on the small strain behavior of residual soils. Although more data are needed for the Kenny Hill formation soil, Figure 11 indicates that the normalized shear modulus versus the shear strain relationship obtained from both the cyclic triaxial test and the shaking table test showed a good agreement despite of a large difference in confining pressure between the two tests. This is somewhat a surprising result for a sandy soil specimen as such behavior is normally observed in clayey soils.

It may be interesting to compare the result of this study with the normalized shear modulus degradation of sandy soil since the soil studied herein is clearly a sandy soil. Oztoprak and Bolton (2013) showed that for sandy soil the normalized shear modulus degradation curves can be represented by two bounds of the curves that are represented by the following equation.

$$G/G_0 = \frac{1}{1 + \left(\frac{\gamma - \gamma_e}{\gamma_r}\right)^a} \quad (1)$$

where γ_e is the characteristic reference shear strain ($=0.0002$ and 0.001 for the lower and upper bounds respectively), a is the curvature parameter ($a=0.88$ for the both bounds), and γ_r is the elastic threshold strain ($= 0$ and 0.00003 for the lower and upper bounds, respectively) beyond which the shear modulus falls below its maximum (Oztoprak and Bolton, 2013). Figure 13 depicts these lower and upper bounds of the degradation curves obtained from Eq. (1). As can be seen from the Figure 13, the test results of this study and Tou (2013) are approximately within these bounds, although some of the data points from the shaking table test of this study and from the Jurong formation are slightly out of the range.

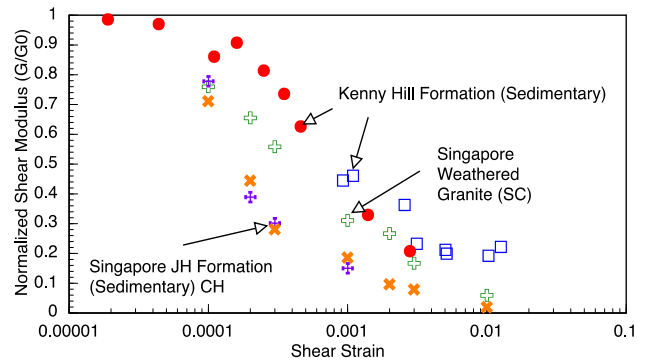


Figure 12 Shear modulus vs. shear strain relationships for different residual soils

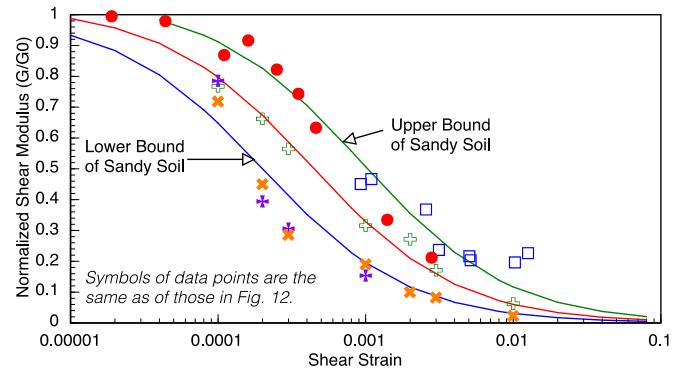


Figure 13 Upper and lower bounds of shear modulus degradation for sand

Therefore, the normalized shear modulus of the residual soils discussed in this study can be evaluated by the degradation curves for sand. The residual soils in tropical region are however consisted of widely different degrees of weathering and different mother rocks, and therefore more efforts are needed to accumulate and integrate the small strain deformation data of the residual soil.

6. CONCLUSION

The following conclusions can be drawn from the results of present experimental studies:

- i) Laboratory testing such as the cyclic triaxial test equipped with the LDT device and the shaking table test with multiple accelerometer measurements can be used to examine the dynamic properties of the residual soil effectively. More improvements and investments are however needed for the test apparatus and practices to achieve higher precisions in the results.
- ii) Although more data are needed for the Kenny Hill formation soil, an agreement was found between the cyclic triaxial test and the shaking table test, despite of a large difference in their confining pressure. This indicates that the compacted residual soil studied herein shows the characteristics of clayey soil, although the sand content of the soil was high (more than 70%) coupled with a high degree of saturation (more than 80%). It was also found that the normalized shear modulus of the residual soils studied herein can be represented by the available degradation curves for sand.
- iii) A comparison was made on the normalized shear modulus degradation curves of the residual soils from similar sedimentary rocks in Malaysia and Singapore. Since the physical and mechanical properties of the residual soils are highly influenced by the process and state of weathering, the shear modulus degradation curves were different between these residual soils despite of the similarity in their parent rock. More efforts are needed to compile and integrate the small strain deformation data of the residual soil.

7. REFERENCES

- Chan, M. Y. (2002) "The influence of wetting on the dynamic properties of completely decomposed granite in Hong Kong". M.Ph. Thesis, Hong Kong University of Science and Technology.
- Chieng, T. S. A. (2013) "Disaster risk reduction in Malaysia and earthquake study based on cyclic triaxial study". B.Eng. Thesis, Universiti Tunku Abdul Rahman.
- Huat, B. B. K., Toll, D. G., and Prasad, A. (2012) "Handbook of Tropical Residual Soils Engineering". CRC Press, Leiden.
- Iwasaki, T., Tatsuoka, F., and Takagi, Y. (1978) "Shear moduli of sands under cyclic torsional shear loading". *Soils & Foundations*, 18, No.1, pp39–50.
- Kazama, M., Toyota, H., Towhata, I., and Yanagisawa, E. (1996) "Stress strain relationship of sandy soils obtained from centrifuge shaking table tests". *Proc. of JSCE*, No. 535/III-34, pp73-82. (in Japanese)
- Kokusho, T. (1980) "Cyclic triaxial test of dynamic soil properties for wide strain range". *Soils & Foundations*, 20, No. 2, pp45–60.
- Lee, T. S. (2013) "Dynamic response of foundation and structure – focused in Kuala Lumpur". B.Eng Thesis, Universiti Tunku Abdul Rahman.
- Leong, E. C., Rahardjo, H., and Cheong H. K. (2003) "Stiffness-strain relationship of Singapore residual soils". *Pacific Conference on Earthquake Engineering*, Poster 12, Paper 160 (www.nzsee.org.nz/db/2003/Print/Paper160p.pdf).
- Ng, C. W. W., and Xu, J. (2012) "Residual soils of Hong Kong".

- Handbook of Tropical Residual Soils Engineering, pp413-461, Ed by Huat, B. B. K. et al., CRC Press, Leiden.
- Osaki, Y. (1994) "Introduction to Spectrum Analysis of Earthquake Motion". Kajima Shuppankai (in Japanese).
- Oztoprak, S., and Bolton, M. D. (2013) "Stiffness of sands through a laboratory test database". *Geotechnique*, Volume 63, No. 1, pp54–70.
- Rahardjo, H., Aung, K. K., Leong, E. C., and Rezaur, R. B. (2004) "Characteristics of residual soils in Singapore as formed by weathering". *Engineering Geology*, Volume 73, pp157–169.
- Toll, D. (2012) "The behavior of unsaturated soil". *Handbook of Tropical Residual Soils Engineering*, pp117-146, Ed by Huat, B. B. K. et al., CRC Press, Leiden.
- Tou, J. H. (2003) "Cyclic triaxial test apparatus for evaluating dynamic properties of residual soils". MSc thesis, Nanyang Technological University.
- Vardanega, P. J., and Bolton, M. D. (2013) "Stiffness of clays and silts: Normalizing shear modulus and shear strain". *J. Geotech. Geoenviron. Eng.*, ASCE, Vol. 139, No. 9, pp1575-1589.
- Vucetic, M., and Dobry, R. (1991) "Effect of soil plasticity on cyclic response". *Journal of Geotechnical Engineering*, ASCE, Vol. 117, No. 1, pp89-107.
- Wong, K. S., Mašin, D., and Ng, C. W. W. (2014) "Modelling of shear stiffness of unsaturated fine grained soils at very small strains". *Computers and Geotechnics*, 56, pp28–39.